

Journal Pre-proofs

Probing Self-assembled Micellar Topologies via Micro-scale Diffusive Dynamics of Surfactants

Alfredo Scigliani, Samuel C. Grant, Hadi Mohammadigoushki

PII: S0021-9797(23)00467-8
DOI: <https://doi.org/10.1016/j.jcis.2023.03.102>
Reference: YJCIS 32000

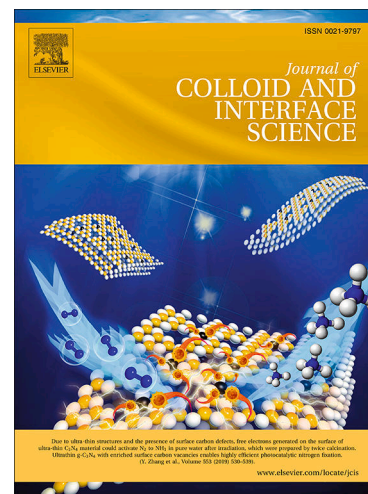
To appear in: *Journal of Colloid and Interface Science*

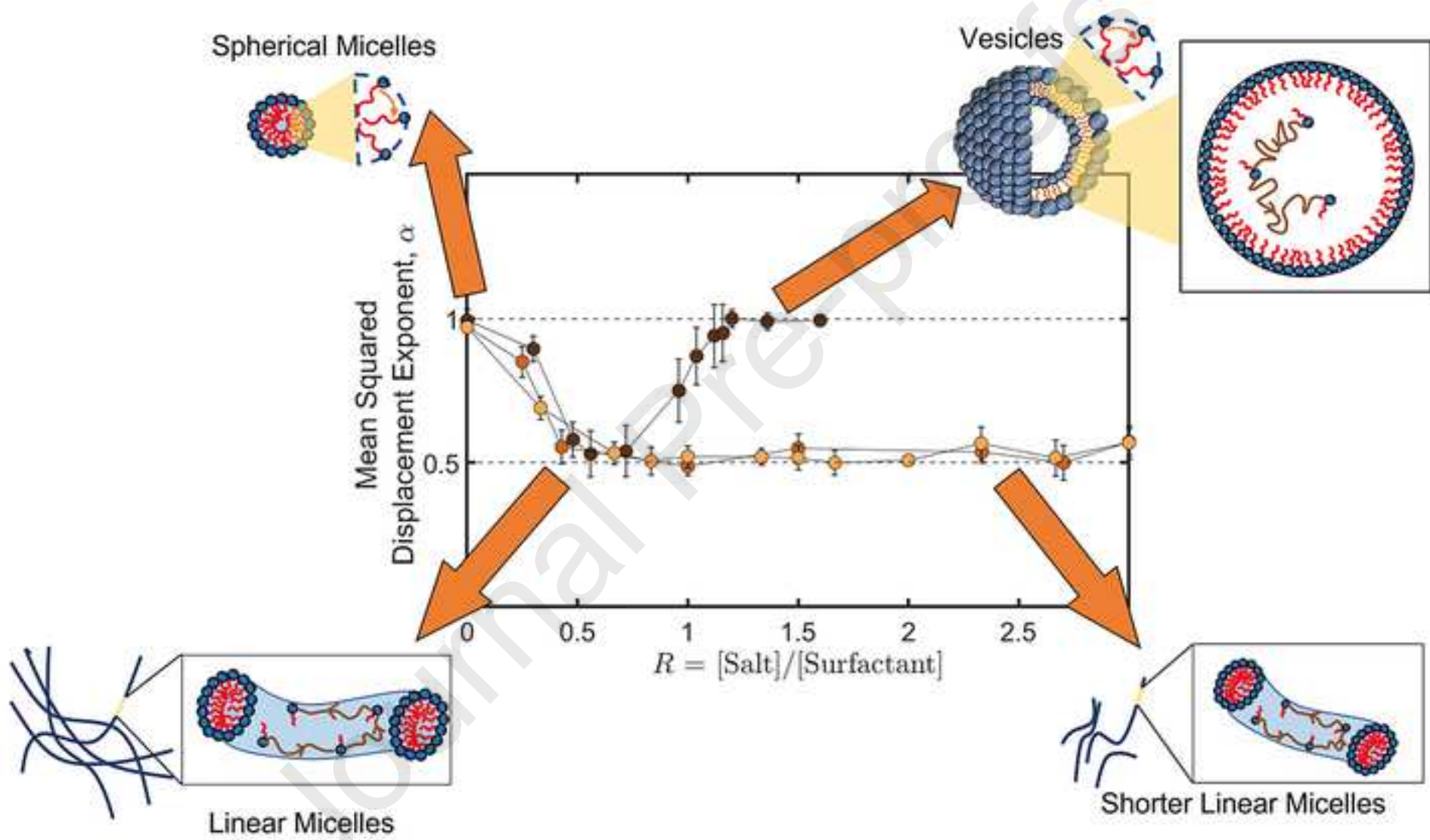
Received Date: 20 January 2023
Accepted Date: 16 March 2023

Please cite this article as: A. Scigliani, S.C. Grant, H. Mohammadigoushki, Probing Self-assembled Micellar Topologies via Micro-scale Diffusive Dynamics of Surfactants, *Journal of Colloid and Interface Science* (2023), doi: <https://doi.org/10.1016/j.jcis.2023.03.102>

This is a PDF file of an article that has undergone enhancements after acceptance, such as the addition of a cover page and metadata, and formatting for readability, but it is not yet the definitive version of record. This version will undergo additional copyediting, typesetting and review before it is published in its final form, but we are providing this version to give early visibility of the article. Please note that, during the production process, errors may be discovered which could affect the content, and all legal disclaimers that apply to the journal pertain.

© 2023 Published by Elsevier Inc.





Probing Self-assembled Micellar Topologies via Micro-scale Diffusive Dynamics of Surfactants

Alfredo Scigliani, Samuel C. Grant,^{a)} and Hadi Mohammadigoushki^{b)}

(Dated: 6 March 2023)

Hypothesis

Surfactants spontaneously self-assemble in aqueous solutions and are critical in energy, biotechnology, and the environment. The self-assembled micelles may experience distinct topological transitions beyond a critical counter-ion concentration, yet the associated mechanical signatures are identical. By monitoring self-diffusion dynamics of individual surfactants in micelles via a non-invasive ^1H NMR diffusometry, we may distinguish various topological transitions overcoming challenges associated with traditional microstructural probing techniques.

Experiments

Three micellar systems based on CTAB/5mS, OTAB/NaOA and CPCl/NaClO₃ are considered at various counter-ion concentrations and their rheological properties are assessed. A systematic ^1H NMR diffusometry is conducted and the resulting signal attenuation is measured.

Findings

With no counter-ion, surfactants self-diffuse freely with a mean squared displacement $Z^2 \sim T_{diff}$ in the micelles. As counter-ion concentration increases, self-diffusion becomes restricted with $Z^2 \sim T_{diff}^\alpha$, and $\alpha \rightarrow 0.5$. Beyond the viscosity peak, for OTAB/NaOA system that shows a linear-shorter linear micelle transition $Z^2 \sim T_{diff}^{0.5}$. Conversely, for the CTAB/5mS system that experiences a linear wormlike-vesicle transition above the viscosity peak, a free self-diffusion is recovered. The diffusion dynamics in CPCl/NaClO₃ are similar to those of OTAB/NaOA. Hence, a similar topological transition is surmised. These results highlight the unique sensitivity of the ^1H NMR diffusometry to micelles topological transitions.

^{a)}grant@magnet.fsu.edu

^{b)}Corresponding Author: hadi.moham@eng.famu.fsu.edu; Department of Chemical and Biomedical Engineering, FAMU-FSU College of Engineering, Tallahassee, FL 32310, USA.; Center for Interdisciplinary Magnetic Resonance, National High Magnetic Field Laboratory, Florida State University, Tallahassee, FL, USA 32310

I. INTRODUCTION

Surfactants are an important class of molecules whose spontaneous self-assembly in aqueous solutions gives rise to a host of interesting nano-structures, including spherical, vesicles, or rodlike in aqueous solutions¹⁻⁵. These self-assembled systems are critical in an array of advanced applications that involve nanomaterials including drug delivery⁶, nano-templating⁷, generating nano-fibers^{8,9} or porous nano-structured materials¹⁰.

In the presence of a counter-ion, these nanoscale colloidal species can further self-assemble into smart and responsive micro-scale wormlike structures that exhibit strong viscoelastic properties¹¹. In a seminal work, Rehage and Hoffman showed that, beyond a critical counter-ion concentration, a peak in the zero-shear viscosity is observed¹². This seemingly anomalous experimental result spurred considerable interest in the scientific community¹³⁻²², and the earliest hypothesis linked the viscosity peak to a topological transition from linear to branched micelles²³. However, it was not until the late 2000s that researchers discovered two additional topological transitions might also exist depending on the chemistry of the surfactant or the counter-ion; linear to shorter linear micelles²⁴ or linear to vesicle micelles²⁵. Due to the critical impact of the topology of the self-assembled micellar system on the performance of these materials, significant efforts have been devoted to establishing a technique and a micro-nano physical interpretation that could help discern the micellar topologies and the associated topological transitions around the viscosity peak. Prime examples include several important articles that employed advanced techniques such as transmission electron microscopy (TEM)²⁶⁻²⁹, neutron spin echo (NSE)³⁰, X-ray photon correlation spectroscopy (XPCS)³¹ or extensional rheology^{22,32,33}.

Despite some advances, these techniques are accompanied by some ambiguities that may render them not suitable for discerning micellar topologies from each other. Besides being expensive and extremely challenging, the sample preparation stage of the TEM imaging may subject the self-assembled micelles to strong flows and inadvertently change their equilibrium topologies^{26-29,34}. In addition, the electrostatic interactions caused by a counter-ion can generate additional effects on the NSE measurements that are difficult to separate from the effects of topological transitions³⁰. In a more recent study, Cho et al.³¹ used a reverse wormlike micellar solution and showed that XPCS did not reveal significant differences between the slow mode segmental dynamics of linear and branched reverse micelles³¹. Finally, techniques based on extensional rheology^{22,32,33} are also invasive and may affect the equilibrium structure of the self-assembled micelles over the course of measurements. Therefore, establishing a robust and non-invasive methodology that is sensitive to the type of micellar topologies and transitions from one to another has remained a critical challenge, mainly due to the limitations of traditional techniques.

Recently, we illustrated that the solution state proton nuclear magnetic resonance (¹H NMR) diffusometry provides unique insights that could be used to successfully distinguish the linear from branched micellar topologies^{35,36}. As noted above, besides the linear-branched micellar topological transition, surfactants may experience other topological transitions depending on their type and salt chemistry; linear to shorter linear micelles²⁴ or linear to vesicles²⁵ around the viscosity peak. More interestingly, the topological transitions are still unresolved for other micellar systems (e.g., cetylpyridinium chloride/sodium chlorate; CPCI/NaClO₃), and attempts at TEM have been unsuccessful³⁷. Therefore, it is still unclear whether ¹H NMR diffusometry is sensitive to any arbitrary micellar topologies and/or

1
2
3
4 associated topological transitions in self-assembled micellar solutions.

5 In this paper, we go beyond the limits of traditional microstructural probing techniques
6 and employ ^1H NMR diffusometry to distinguish various micellar topologies and topological
7 transitions from each other besides the linear-branched transition. By monitoring and track-
8 ing the self-diffusion of individual surfactant molecules in nanoporous self-assembled micelles,
9 we aim to obtain detailed information that could be used toward identifying different types of
10 micellar topologies for the first time. For this purpose, we used two self-assembled micellar
11 systems based on cetyltrimethylammonium bromide/ 5-methyl salicylate (CTAB/5mS)²⁵,
12 and octyl trimethylammonium bromide/sodium oleate (OTAB/NaOA)²⁴ that have been re-
13 ported to exhibit either a linear-to-vesicle and linear-to-shorter linear micelle transitions
14 beyond the viscosity peak, respectively. In addition, we assessed the micro-scale diffusion
15 dynamics of surfactants in a system based on CPCI/NaClO₃ and directly compared the
16 results with other systems, which in turn allows us to identify the nature of topological
17 transitions in the latter system.
18
19
20
21
22

23 II. EXPERIMENTAL

24 A. Materials:

25
26
27
28 Three self-assembled micellar solutions were made: The first one consists of Cetyl-
29 trimethylammonium Bromide (CTAB) and 5-methyl-salicylic acid (5mS) in 99.9% Deu-
30 terium Oxide (D₂O). Both CTAB and 5mS were obtained from Sigma-Aldrich and the D₂O
31 from Cambridge Isotopes Laboratories. This system is made at a fixed CTAB concentration
32 of 12.5mM while the salt-to-surfactant concentration ratio (R) varies from 0 to 1.60. The
33 second system consists of octyl-trimethylammonium Bromide (OTAB) and Sodium Oleate
34 (NaOA) in D₂O. Both OTAB and NaOA were obtained from Tokyo Chemical Industry
35 (TCI). Although both OTAB and NaOA are surfactants, for the purpose of comparison
36 with other systems, the systematic study consisted in varying the ratio (R) of OTAB and
37 NaOA, maintaining the total concentration in the solution of 3 wt %. Finally, the third
38 system consisted of Cetyl-pyridinium Chloride (CPCI) and Sodium Chlorate (NaClO₃) in
39 D₂O. Both CP_{*y*}Cl and NaClO₃ were obtained from Sigma-Aldrich. This system's surfac-
40 tant (CPCI) concentration was kept fixed at 0.3M while covering R values from 0 to 3. All
41 chemicals were used as received.
42
43
44
45
46

47 B. Fluid Characterizations:

48
49
50 All experiments in this study for CTAB/5mS and OTAB/NaOA were conducted at a
51 temperature $T = 25^\circ\text{C}$ and $T = 32^\circ\text{C}$ for CPCI/NaClO₃ system. To confirm the transitions
52 in morphology associated with the viscosity peak, we have measured the zero-shear rate
53 viscosity of the solutions via a commercial rheometer (Anton-Paar model MCR-302) and a
54 cone-and-plate geometry. The cone used had a diameter of 50 mm and an angle of 1° .
55
56
57

58 C. NMR Diffusometry:

59
60 ^1H NMR diffusometry was performed to probe the self-diffusion dynamics of the sur-
61 factant molecules in the micellar solutions. We used the 21.1-T ultra-widebore magnet
62
63
64
65

equipped with Resonance Research Inc gradients (64-mm ID) coupled to Bruker Biospin 60-A Great60 amplifiers accessible through the National High Magnetic Field Laboratory. The magnet was equipped with a 900-MHz Bruker NEO console, capable of performing solid-state, liquid-state, and microimaging experiments. The measurements were performed in a 5mm ^1H linear birdcage with the surfactant solutions placed in sealed 5 mm NMR tubes. As in a previous study³⁵, ^1H NMR spectra were acquired with a diffusion-weighted stimulated echo (DW-STEAM; see details in³⁵.) Protons (^1H) were used as the probe in order to increase the overall NMR signal-to-noise ratio (SNR). In order to characterize the diffusion behavior, separate experiments with eight diffusion delay Δ times (17, 22, 52, 102, 202, 302, 402, and 502 msec) were carried out. Using 32 different values of gradient magnetic field strength ($g = 0\text{-}754.6$ mT/m) to vary the diffusion weighting while maintaining a fixed pulse gradient duration (δ) of 6 ms. These parameters covered diffusion times (T_{diff}) ranging from 15 to 500 ms and q values from 0 to 0.095 $1/\mu\text{m}$. The post-processing of the diffusion-weighted data is identical to our previous publications and discussed therein^{35,36}.

III. RESULTS AND DISCUSSION:

A. Rheology:

We begin our experiments by characterizing the rheology of the self-assembled micellar solutions. Fig. 1 shows the zero-shear viscosity as a function of the salt-to-surfactant concentration ratio (R) for the three self-assembled micellar solutions. As expected, the zero-shear viscosity increases as R increases until it reaches a maximum value at a critical salt concentration. Beyond this critical point, further increase of the salt concentration gives rise to a decline in the zero-shear viscosity, which is consistent with the existing literature^{24,25,38}.

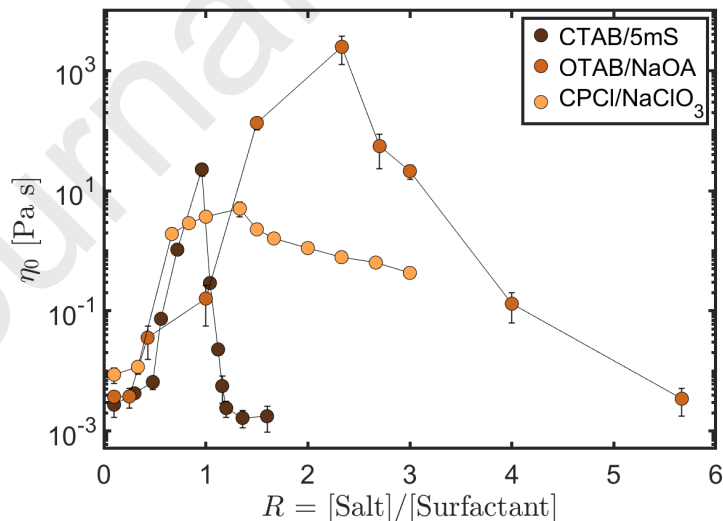


FIG. 1. Zero-shear viscosity as a function of salt to surfactant concentration ratio, R . The maximum viscosity corresponds to $R = 0.96$ in CTAB/5mS, $R = 2.33$ in OTAB/NaOA, and $R = 1.33$ in CPCI/NaClO₃ systems. For data points where error bars are not seen, the measured error was less than the marker size.

B. ^1H NMR diffusometry:

Following fluid characterization, proton (^1H) NMR spectroscopy and diffusometry experiments were conducted. In principle, in a self-assembled micellar system, proton self-diffusion can be associated with the diffusion of four different sources: the medium molecules (in this case due to the presence of a small amount of water in D_2O), salt, surfactant, and/or the self-assembled micelles themselves. Because individual surfactants, salt, or water molecules are much smaller than the self-assembled micelles, self-diffusion is dominated by the individual molecules.

Fig. 2 shows the NMR spectra of the three micellar solutions used in this study. These spectra were collected at different diffusion weighting B following the application of a DW-STEAM sequence (see details in experiments). Table (III B) below lists the chemical resonances associated with each species. As expected, the NMR signal intensity decreases as a function of diffusion weighting (B ; see details below) for all systems. Because chemical resonances associated with each molecule are distinct, the signal attenuation of each chemical shift allows us to assess the self-diffusion of each species in the solution separately. In the following, we will first assess the diffusion of proton in the medium (residual water in the D_2O) and then assess the self-diffusion mechanism of the individual surfactant molecule. Because salt molecules are strongly associated with surfactants, their self-diffusion dynamics are similar to those of surfactants. Therefore, for brevity, we only present the diffusion dynamics of surfactants in self-assembled micellar solutions (sample plots showing diffusion dynamics of salt are provided in Fig. S1 and Fig. S2 of the supplementary materials).

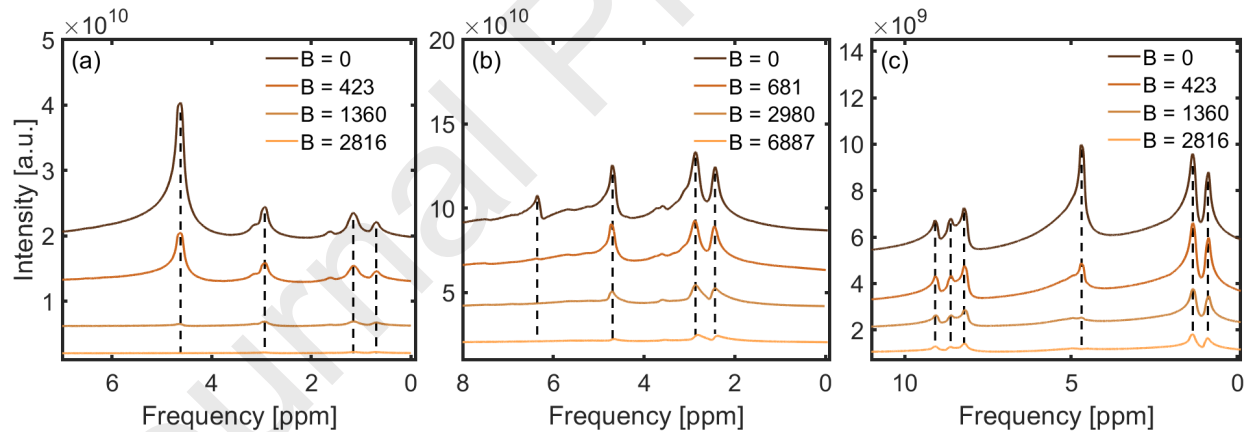


FIG. 2. NMR spectra as a function of frequency for (a) CTAB/5mS, (b) OTAB/NaOA, and (c) CPCl/NaClO₃ micellar solutions. For the chemical resonances associated with each peak, refer to Table I.

Water Self-diffusion

As noted in Table I, the chemical resonance associated with the residual protons of the water molecules resides at 4.7 ppm. Although we used D_2O as the medium for the surfactant solutions, due to the presence of some residual water in the D_2O , this peak appears in the NMR spectra. Fig. 3 (a) shows the normalized signal attenuation associated with the protons of the water molecules as a function of the B value in sample micellar systems. This behavior

System	Chemical Shifts [ppm]	Molecule
CTAB/5mS	2.9 ³⁹	(CH ₂) _n (Surfactant)
	0.7 ³⁹	ω-CH ₃ (Surfactant)
	1.16 ⁴⁰	Methyl salicylate ion (Salt)
OTAB/NaOA	2.8 ⁴¹	(CH ₂) _n (Surfactant)
	2.5 ⁴¹	ω-CH ₃ (Surfactant)
	6.3 ⁴²	Oleic acid ion (Salt)
CPCl/NaClO ₃	1.3, 0.86 ⁴³	ω-CH ₃ (Surfactant)
	8.2 ⁴⁴	Meta-CH (Surfactant)
	8.5 ⁴⁴	Para-CH (Surfactant)
	9.0 ⁴⁴	Ortho-CH (Surfactant)
D ₂ O medium	4.7 ⁴⁵	¹ H (Water)

TABLE I. Chemical resonances associated with different species in the wormlike micellar solutions used in this study.

is expected for Brownian (free) self-diffusion of a molecule. In a series of papers, Stejskal and Tanner described the use of pulsed magnetic field gradients to assess the free and restricted self-diffusion of species in a medium^{46,47} and illustrated that for a free self-diffusion, the NMR signal attenuation follows a mono-exponential type decay:

$$S(B)/S(0) = \exp(-B \cdot ADC). \quad (1)$$

Here S represents the NMR signal intensity, B is the diffusion weighting, and ADC is the

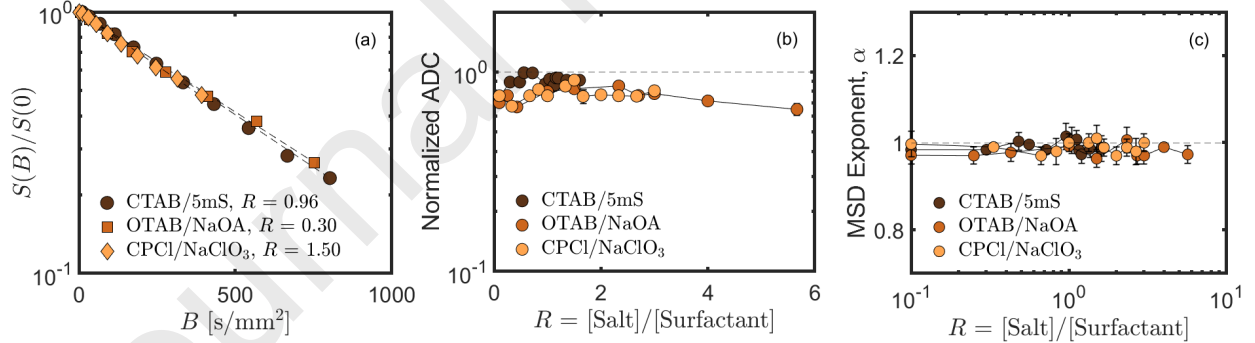


FIG. 3. (a) NMR Signal attenuation as a function of diffusion weighting B for water molecules in three surfactant systems. (b) Normalized apparent diffusion coefficient (ADC) as a function R . The calculated diffusion coefficients are normalized by the diffusion coefficients reported for water molecules in water, $1.872 \times 10^{-9} \text{ m}^2/\text{s}$ for 25°C and $2.189 \times 10^{-9} \text{ m}^2/\text{s}$ for 32°C .⁴⁸ (c) MSD exponent α associated with water proton diffusion in micellar solutions.

diffusion coefficient. $B = 0$ is the reference state for no diffusion weighting. The diffusion weighting $B = (\gamma \delta g)^2 T_{diff}$, where $\gamma = 2.67 \times 10^8 \text{ rad}/(\text{s T})$ is the gyromagnetic ratio of the proton, the parameter δ represents the time duration of the gradient pulse, and g is the strength of the magnetic gradient, which is incremented to vary the diffusion weighting. Moreover, $T_{diff} = \Delta - \delta/3$ denotes the diffusion time in the DW-STEAM sequence (see experiments for more details). The dashed lines in Fig. 3(a) show the best fit to Eq. (1),

which is used to calculate the apparent diffusion coefficient of the water in these micellar systems. Fig. 3 (b) shows the ratio of the water diffusion coefficients obtained in this work normalized by the reported diffusion coefficient of water in the published literature⁴⁸. Consistent with our previous measurements in other surfactant systems, the diffusion of water in self-assembled micellar systems is slower than its self-diffusion in pure H₂O³⁵. The slower proton self-diffusion in micellar solutions is probably caused by micelles that could obstruct the diffusion of protons in the bulk D₂O or hydration of the protons to the micelles that could lower the mobility of the protons in self-assembled micellar solutions.

Alternatively, the self-diffusion of molecules in any medium could be described by the following relation:

$$S(q)/S(0) = \exp\left(-\frac{1}{2}Z^2q^2\right), \quad (2)$$

where $Z^2 \propto (\Delta - \delta/3)^\alpha$ is the mean squared displacement of the molecules and $q = \gamma\delta g$. The α parameter may be used to assess the nature of self-diffusion (whether restricted or free) in a medium. For example, it is very well-known that a Brownian type (free) self-diffusion gives rise to $\alpha = 1$ ⁴⁹. Fig. 3(c) shows the α exponent associated with the diffusion of water molecules for the entire range of salt-to-surfactant concentration ratios for the three surfactant systems. As expected, the self-diffusion of water molecules is well-described by a Brownian-type diffusion with $\alpha = 1 \pm 0.02$.

Self-diffusion of Surfactants

Self-diffusion of surfactants is far more complex than the residual protons of the water molecules. Although in the absence of salt $R \rightarrow 0$, surfactants self-diffuse in a free manner, their self-diffusion in the presence of a counter-ion ($R > 0$) slows significantly and becomes restricted. This restriction is manifested by a significant deviation from a mono-exponential decay at high B values (see sample plots in Fig. S3 of the supplementary materials). In principle, surfactant molecules are strongly associated with their micelles, and their self-diffusion in micellar solutions should be restricted within the micelles themselves, provided that they self-diffuse to long distances (or high B values) to notice the presence of the restriction. Thus, their self-diffusion could occur in the transverse direction (cross-section of the micelles) or in the axial direction (along the contour length of the micelle). In fact, for a similar problem that involves self-diffusion of water molecules in randomly oriented capillary tubes, Callaghan and co-workers showed that the following relation theoretically can describe the NMR signal attenuation⁵⁰:

$$S(B)/S(0) = \exp(-BD_\perp) \int_0^1 \exp(-B[D_\parallel - D_\perp]x^2) dx \quad (3)$$

Here, D_\parallel and D_\perp denote the axial and transverse diffusion coefficients of water molecules in the capillary tubes. Eq. (3) provides a general solution that could be applied to restricted and/or free self-diffusion. For example, if $D_\parallel = D_\perp = D$, this model predicts a mono-exponential signal decay, and therefore, a free self-diffusion behavior is expected. However, if $D_\parallel \neq D_\perp$, the self-diffusion becomes restricted (and could be 1D or 2D). Therefore, as a first attempt, we used the model proposed by Callaghan and co-workers to assess the ADCs associated with the surfactants in different micellar systems (see solid curves in Fig. S3 of

the supplementary materials). Despite the high quality of the fit to the experimental data, we uncovered an issue that pertains to the values of diffusion coefficients obtained from fitting to this model. In several instances, the numerical values of the diffusion coefficients are not meaningful. Table SI in the supplementary material shows the numerical values of the diffusion coefficients found for some of the surfactant solutions. Note that in several instances, the diffusion coefficient turns out to be larger than the ones calculated for the protons of the water molecules suggesting that surfactants self-diffuse faster than water molecules, which is clearly inconsistent with the signal attenuation behavior. Note that the peak associated with the water molecule decays much more rapidly than the surfactant molecules (cf. Fig. 3(a) and Fig. S3). Therefore, ADCs for surfactant molecules should be much smaller than those measured for residual protons of D₂O. For other systems, the best fit to the experimental data yields a negative value for the diffusion coefficients. The issues with the fit to Callaghan’s model could arise from differences between our system and those studied by Callaghan and co-workers⁵⁰. Particularly in our experiments, surfactants are strongly associated and bound to the micelles due to the presence of electrostatic attractions. In Callaghan’s approach, molecules are not associated with capillaries through any attractive potentials (e.g., electrostatic attractions between the diffusive molecule and the boundary).

Because of the aforementioned issues with the fit to the Callaghan model, an alternative model was fitted to the experimental data. Ideally, the model considered for this purpose should capture the underlying physics involved in the restricted diffusion of surfactants in micellar tubes and produce physically meaningful ADCs. Individual surfactant molecules self-diffuse through nano and micro-porous wormlike micelles structures that may resemble the porous structure of biological tissues (e.g., brain or nerves). Previous studies in such biological environments have shown that intracellular water diffusion displays non-monoexponential diffusion decays, and can be fitted with a slow exchange model to report fast and slow ADCs⁵¹⁻⁵³ over a range of diffusion times. In our experiments, we observed a similar signal decay and elected to fit this decay to a bi-exponential function as both a model fit to generate reasonable ADCs and a probe of different micellar conditions. The bi-exponential decay function is given as:

$$S(B)/S(0) = \xi \exp(-BD_f) + (1 - \xi) \exp(-BD_s). \quad (4)$$

Where D_s and D_f are slow and fast diffusion coefficients for micellar systems, respectively, and ξ is the pool fraction associated with the fast diffusion coefficient. We hypothesize that these two diffusion coefficients are similar if the micelles’ topology is symmetric (e.g., spherical or vesicle) or vastly different if the micelles form asymmetric shapes (e.g., cylindrical or wormlike), providing a criterion to distinguish topological transitions from each other.

Fig. 4 shows a series of superimposed NMR signal attenuation at different salt-to-surfactant concentration ratios for the three surfactant systems. We first begin our discussion by describing the signal attenuation at $R = 0$. In the absence of any salt, all three systems indicate a free self-diffusion (or a mono-exponential decay) for surfactant molecules, which is expected (see left column of Fig. 4 and $R = 0$). For larger R values below the viscosity peak, where we expect rod-like micelles to form, a clear deviation from mono-exponential type signal decay ($D_f \neq D_s$) is observed (see left column of Fig. 4). The three systems behave similarly for R values slightly above the maximum viscosity peak (see the middle column of Fig. 4), which is expected because all these systems still contain a large amount of linear wormlike micelles. Deviations between these systems start to appear at

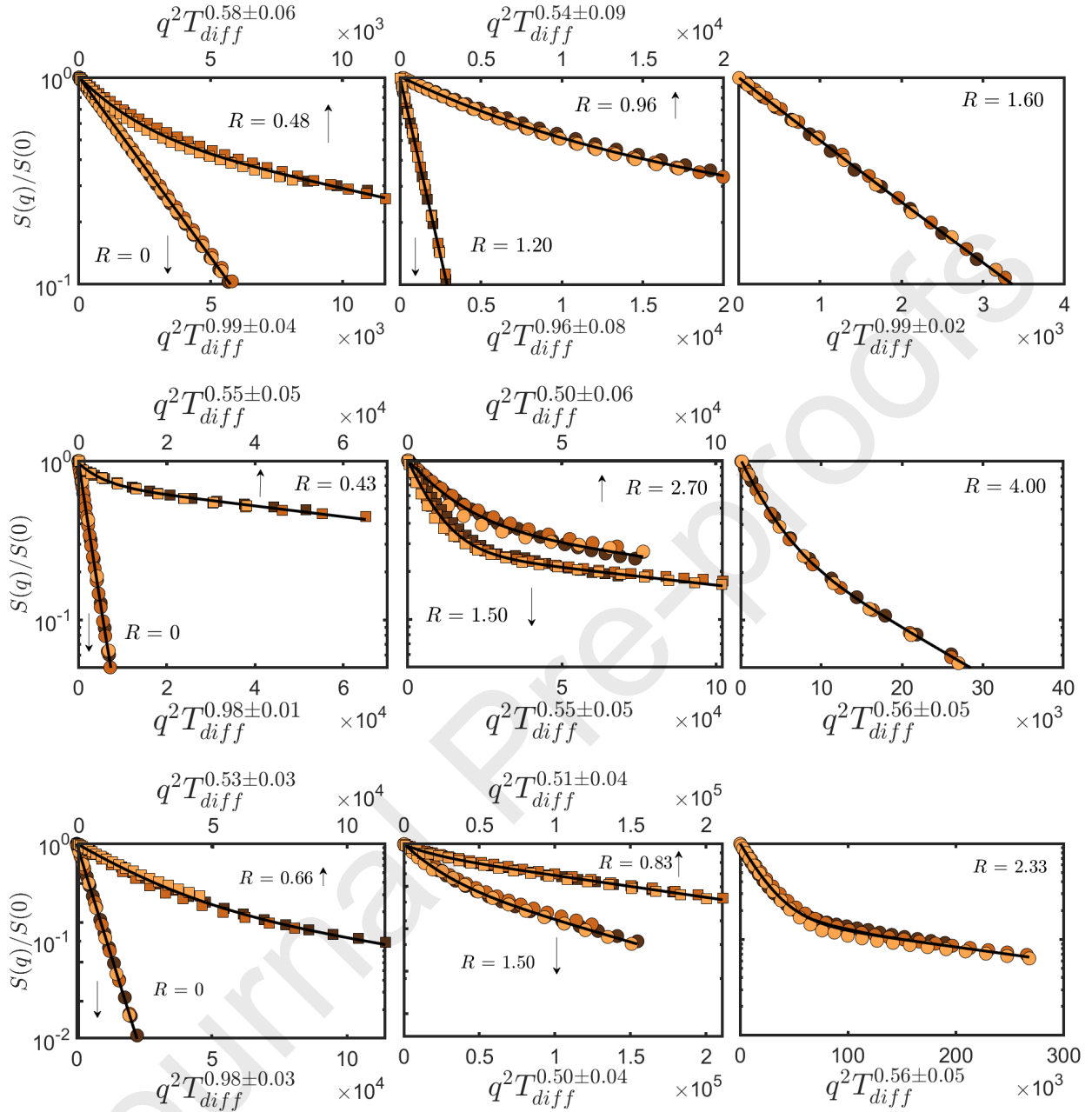


FIG. 4. Normalized NMR signal attenuation of surfactant peaks. The top, middle, and bottom rows show the data for CTAB/5mS, OTAB/NaOA, and CPCl/NaClO₃ solutions, respectively. Each color corresponds to a different diffusion time T_{diff} : brown (50 ms), orange (200 ms), and yellow (500 ms). The solid black curves correspond to the best fit of Eq. (4) to the experimental data. The arrows are guides indicating which horizontal axis the data sets correspond to.

larger salt-to-surfactant concentration ratios beyond the viscosity peak. While signal attenuation becomes mono-exponential for the CTAB/5mS system, for the two other systems, it remains restricted (i.e., significantly deviating from mono-exponential decay) even at the highest salt-to-surfactant concentration ratios (see right column of Fig. 4 for three systems).

To further analyze this data, we have fitted the bi-exponential function to the experimen-

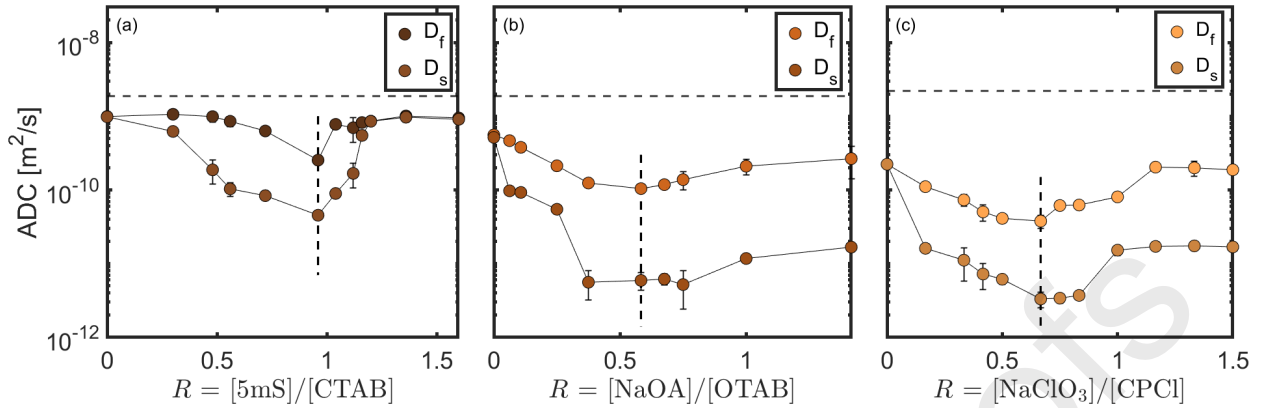


FIG. 5. Apparent Diffusion Coefficient in terms of salt-to-surfactant concentration ratio for a) CTAB/5mS, b) OTAB/NaOA, and c) CPCl/NaClO₃. The vertical dashed line denotes the concentration at which the maximum zero-shear viscosity is observed.

tal data, and the resulting ADCs are plotted in Fig. 5. The reported ADC values of Fig. 5 are obtained by averaging the measured ADC values for $\Delta \geq 200$ ms. In fact, the ADC values depend on the diffusion delay time (T_{diff}). At small diffusion delay times, the ADC values are high, and as the diffusion delay increases, the ADC decreases until it levels off beyond a diffusion delay of 200ms (see Fig. S4 in the supplementary materials). This result is consistent with our previous measurements³⁵ and can be rationalized as follows: At short diffusion delay times, the surfactant molecules self-diffuse to short distances such that they are not affected by restrictions (or micelle walls). However, as the diffusion delay time increases, surfactant molecules self-diffuse to farther distances, and therefore, their self-diffusion is affected by the micelles restrictions. Fig. 5 shows that the apparent diffusion coefficients are similar at low salt-to-surfactant concentration ratios because a mono-exponential type decay best fits the experimental data. The mono-exponential signal decay also suggests that the micellar shape should be symmetric. Note that surfactant concentration is well beyond critical micelle concentration (CMC). Therefore, in the absence of a counter-ion, the self-assembled micelles are expected to form symmetric (or spherical) shapes. As the salt-to-surfactant concentration ratio increases, these two ADCs become vastly apart, indicating the growth of one micelles dimension, increasing their asymmetry. Interestingly, while for CTAB/5mS system, the self-diffusion once again becomes mono-exponential at higher salt-to-surfactant concentration ratios, for the OTAB/NaOA system, the deviations between these two ADCs remain significant well beyond the viscosity peak. These results suggest that while micellar asymmetry disappears in CTAB/5mS solution, micelles of OTAB/NaOA remain highly asymmetric (rod-like with a high aspect ratio) well beyond the viscosity peak. Finally, a closer look at the Fig. 5 (c) on CPCl/NaClO₃ system reveals that similar to OTAB/NaOA solution, the self-diffusion of surfactant molecules remains restricted (with ADCs deviating significantly) well above the viscosity peak. Hence, we can surmise from these results that the micellar solutions based on CPCl/NaClO₃ should experience a similar topological transition to those reported for OTAB/NaOA beyond the viscosity peak; a linear-to-shorter linear micellar transition.

The diffusion data are further analyzed by monitoring the variations of the mean squared displacement (Z^2) as a function of diffusion time (T_{diff}). Fig. 6(a) highlights the most

important results of this study. As the salt-to-surfactant concentration ratio increases, the MSD exponent α decreases for three systems in a similar manner and approaches $\alpha \approx 0.5$ around the critical salt-to-surfactant concentration ratios (see also Fig. 6(b)). At $R = 0$, surfactants concentration is beyond CMC, and therefore, the micellar solutions consist of a mixture of spherical micelles and some individual surfactants. The diffusion of this mixture is well described by a free-self diffusion for which $\alpha \approx 1$. As the salt concentration increases, spherical micelles begin to undergo a geometrical transition to rod-like micelles. At very low salt concentrations (e.g., $R = 0.2-0.3$), it is possible that a significant fraction of micelles is still spherical due to a lack of enough salt to screen out electrostatic repulsion between all surfactants that exist in the solution. The self-diffusion of surfactants or the self-diffusion of spherical micelles in D_2O would produce $\alpha \approx 1$, while self-diffusion of surfactants in rod-like micelles is expected to generate $\alpha \approx 0.5$ ⁵⁴. Therefore, an intermediate α value of $\approx 0.7 - 0.8$ in the low salt concentration regime suggests that there exists a mixture of spherical and rod-like micelles in the solution at very low salt concentrations. This sub-diffusive behavior (i.e., $\alpha < 1$) is similar to the results of molecular dynamics (MD) simulations of Dhakal and Sureshkumar⁵⁵ for a surfactant system based on cetyl-trimethyl-ammonium chloride (CTAC) and salicylate ions. Dhakal and Sureshkumar showed that for fairly low salt-to-surfactant concentration ratios with $R = 0.2$, $\alpha \approx 0.74$ ⁵⁵.

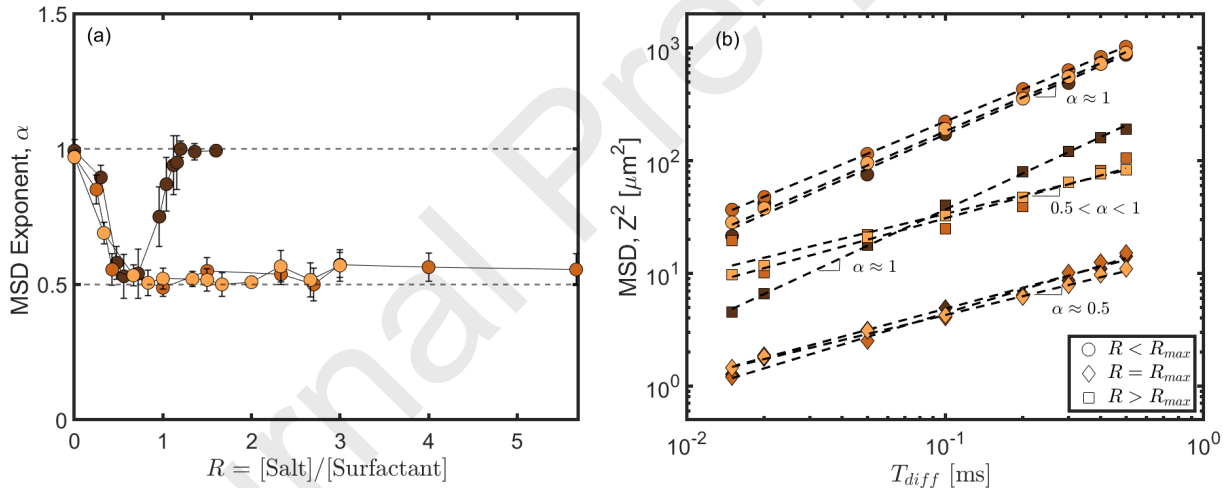


FIG. 6. (a) mean squared displacement exponent (α) as a function of the salt-to-surfactant concentration ratio, R for three micellar systems. (b) MSD (Z^2) as a function of diffusion time (T_{diff}) at different salt-to-surfactant concentration ratios (R). Circles, squares, and diamonds correspond to experimental data sets at salt-free, relatively low R , and relatively higher R values. Here R_{max} denotes the critical salt to surfactant concentration at which a viscosity peak is observed. In part (b), light-to-dark color symbols correspond to CPCl/NaClO₃, OTAB/NaOA, and CTAB/5mS, respectively. The least-squared error (coefficient of determination) for these fittings is beyond 0.990 for all datasets.

As the salt concentration increases and the rod-like micelles become the dominant micellar shape, $\alpha \rightarrow 0.5$ (see Fig 6(b)). In a combined theoretical and experimental study, Angelico et al.⁵⁴ showed that $\alpha = 0.5$ is associated with the curvilinear diffusion of surfactant molecules along the contour length of the wormlike micelles. Consequently, we suggest that the curvilinear diffusion of individual surfactants along the longest axis of the linear

wormlike micelles is the dominant surfactant self-diffusion mechanism around the viscosity peak in our experiments. Beyond the critical salt-to-surfactant concentration ratio, these systems show distinct responses. While for CTAB/5mS system α increases towards the free self-diffusion of surfactants ($\alpha \approx 1$) at higher salt to surfactant concentrations, it levels off around $\alpha \approx 0.5 \pm 0.05$ for OTAB/NaOA and CPCI/NaClO₃ systems (see also Fig. 6(b)). The latter results suggest that while CTAB surfactants diffuse freely inside micelles with a symmetric shape (in this case, vesicles), OTAB and CPCI surfactants diffuse curvilinearly inside linear micellar tubes. This interpretation is in line with the published literature on the topology of the micelles in these systems^{24,25} and gives further credence to ¹H NMR diffusometry as a robust and non-invasive technique that could unambiguously predict the micelle's topologies and topological transitions in self-assembled systems.

Finally, we note that in their MD simulations, Dhakal and Sureshkumar recovered a super-diffusive behavior with α sometimes reaching as high as $\alpha \approx 2$ for high R values⁵⁵. These authors linked the super-diffusive behavior to the dynamics of branched points in the micellar solutions⁵⁵. In the experiments reported in this paper, we did not observe a super-diffusive behavior for any of the surfactant systems. This is unsurprising because none of the surfactant systems used in this study are expected to form branched points.

Although we have successfully developed a technique and insights towards distinguishing different micellar topological transitions, a lingering open fundamental question in the field is the underlying physics causing different topological transitions in micelles. It is our hypothesis that salt and counter-ion chemistry may introduce solvency effects and change the ionic strength of the solution, which may in turn affect micelles stiffness, length, and possibly their topological transitions^{56,57}. Molecular dynamic simulations provide a unique opportunity to assess the impact of surfactant and salt chemistry on topological transitions in various micellar solutions.

IV. CONCLUSIONS

In summary, by probing the restricted diffusion of individual surfactant molecules within nano and micro-porous micellar structures, we successfully assessed the topological transitions in three self-assembled micellar solutions with different chemistries. Our results indicate that a bi-exponential signal attenuation function with two ADCs fits best over the entire range of salt-to-surfactant concentration ratios (Fig. 4). As the salt-to-surfactant concentration ratio increases to the viscosity peak, the deviation between the two ADCs becomes significant, indicating a geometrical asymmetry in the micellar shape (Fig. 5). In addition, the MSD exponent α decreases below unity and approaches $\alpha \approx 0.5$ for these micellar systems (Fig. 6(a)). Interesting differences arise between these systems for salt concentrations beyond the viscosity peak. For CTAB/5mS, the deviation between ADCs decreases until it disappears at high salt-to-surfactant concentration ratios, and the α parameter increases towards unity (Fig. 6(a)). Conversely, for the OTAB/NaOA solution, the ADCs remain significantly different, and the α parameter levels off around 0.5 for salt to surfactant concentrations beyond the viscosity peak (Fig. 6(a)). Finally, the diffusion dynamics of the surfactant in CPCI/NaClO₃ solution are similar to those measured for the OTAB/NaOA system. These results clearly indicate that while the nature of topological transitions above the viscosity peak in CTAB/5mS and OTAB/NaOA should be different, the system based on CPCI/NaClO₃ is expected to experience the same topological transition as that reported for the OTAB/NaOA solution; a linear to shorter linear micellar transition.

The outcomes of this paper demonstrate that ^1H NMR diffusometry is a non-invasive, robust, and simple technique that not only overcomes challenges associated with TEM or scattering-based techniques but it can successfully predict and distinguish a variety of self-assembled micellar topologies and topological transitions. Although this study was restricted to three micellar systems, it is anticipated that this method could be extended to other self-assembled surfactant solutions, including reverse micellar solutions³¹, mixed surfactant solutions⁵⁸ or polymer micelle solutions⁵⁹.

V. ACKNOWLEDGEMENTS

This work was partially performed at the US National High Magnetic Field Laboratory (NHMFL), which is supported by the State of Florida and the National Science Foundation Cooperative Agreement No. DMR-1644779. In addition, we acknowledge support from the National Science Foundation through award CAREER CBET 1942150 for the funding of this study. SCG is supported by the NIH (R01-NS102395 and R01-NS072497). Grant and Mohammadigouski serve as co-senior authors of this work.

REFERENCES

- ¹Joshua J Cardiel, Lige Tonggu, Alice C Dohnalkova, Pablo De La Iglesia, Danilo C Pozzo, Ligu Wang, and Amy Q Shen. Worming their way into shape: Toroidal formations in micellar solutions. *ACS nano*, 7(11):9704–9713, 2013.
- ²S Ezrahi, E Tuval, and A Aserin. Properties, main applications and perspectives of worm micelles. *Advances in colloid and interface science*, 128:77–102, 2006.
- ³Cecile A Dreiss. Wormlike micelles: where do we stand? recent developments, linear rheology and scattering techniques. *Soft Matter*, 3(8):956–970, 2007.
- ⁴Toyoko Imae, Ritsu Kamiya, and Shoichi Ikeda. Formation of spherical and rod-like micelles of cetyltrimethylammonium bromide in aqueous nabr solutions. *Journal of colloid and interface science*, 108(1):215–225, 1985.
- ⁵Jacob N Israelachvili. *Intermolecular and surface forces*. Academic press, 2011.
- ⁶S Chauhan, Kuldeep Singh, and CN Sundaresan. Physico-chemical characterization of drug-bio-surfactant micellar system: a road for developing better pharmaceutical formulations. *Journal of Molecular Liquids*, 266:692–702, 2018.
- ⁷Bing Tan, Alan Dozier, Hans-Joachim Lehmler, Barbara L Knutson, and Stephen E Rankin. Elongated silica nanoparticles with a mesh phase mesopore structure by fluorosurfactant templating. *Langmuir*, 20(17):6981–6984, 2004.
- ⁸Guicun Li and Zhikun Zhang. Synthesis of dendritic polyaniline nanofibers in a surfactant gel. *Macromolecules*, 37(8):2683–2685, 2004.
- ⁹Kyung-Soo Moon, Ho-Joong Kim, Eunji Lee, and Myongsoo Lee. Self-assembly of t-shaped aromatic amphiphiles into stimulus-responsive nanofibers. *Angewandte Chemie International Edition*, 46(36):6807–6810, 2007.
- ¹⁰Daiwon Choi and Prashant N Kumta. Surfactant based sol-gel approach to nanostructured lifepo4 for high rate li-ion batteries. *Journal of Power Sources*, 163(2):1064–1069, 2007.
- ¹¹Ashish V Sangwai and Radhakrishna Sureshkumar. Coarse-grained molecular dynamics

- 1
2
3
4 simulations of the sphere to rod transition in surfactant micelles. *Langmuir*, 27(11):6628–
5 6638, 2011.
- 6
7 ¹²H Rehage and H Hoffmann. Rheological properties of viscoelastic surfactant systems. *The*
8 *Journal of Physical Chemistry*, 92(16):4712–4719, 1988.
- 9
10 ¹³Ignatius A Kadoma, Caroline Ylitalo, and Jan W van Egmond. Structural transitions in
11 wormlike micelles. *Rheologica Acta*, 36(1):1–12, 1997.
- 12
13 ¹⁴Vania Croce, Terence Cosgrove, Geoff Maitland, Trevor Hughes, and Göran Karlsson.
14 Rheology, cryogenic transmission electron spectroscopy, and small-angle neutron scattering
15 of highly viscoelastic wormlike micellar solutions. *Langmuir*, 19(20):8536–8541, 2003.
- 16
17 ¹⁵Zhiqing Lin, Bin Lu, Jacques L Zakin, Yeshayahu Talmon, Yi Zheng, H Ted Davis, and
18 LE Scriven. Influence of surfactant concentration and counterion to surfactant ratio on
19 rheology of wormlike micelles. *Journal of colloid and interface science*, 239(2):543–554,
20 2001.
- 21
22 ¹⁶Gregoire Porte, Jacqueline Appell, and Yves Poggi. Experimental investigations on the
23 flexibility of elongated cetylpyridinium bromide micelles. *The Journal of Physical Chem-*
24 *istry*, 84(23):3105–3110, 1980.
- 25
26 ¹⁷G Porte, R Gomati, O El Haitamy, J Appell, and J Marignan. Morphological transfor-
27 mations of the primary surfactant structures in brine-rich mixtures of ternary systems
28 (surfactant/alcohol/brine). *The Journal of Physical Chemistry*, 90(22):5746–5751, 1986.
- 29
30 ¹⁸Beth A Schubert, Eric W Kaler, and Norman J Wagner. The microstructure and rheology
31 of mixed cationic/anionic wormlike micelles. *Langmuir*, 19(10):4079–4089, 2003.
- 32
33 ¹⁹C Oelschlaeger, M Schopferer, Frank Scheffold, and N Willenbacher. Linear-to-branched
34 micelles transition: A rheometry and diffusing wave spectroscopy (dws) study. *Langmuir*,
35 25(2):716–723, 2009.
- 36
37 ²⁰Danila Gaudino, Rossana Pasquino, and Nino Grizzuti. Adding salt to a surfactant so-
38 lution: Linear rheological response of the resulting morphologies. *Journal of Rheology*,
39 59(6):1363–1375, 2015.
- 40
41 ²¹D Danino, A Bernheim-Groswasser, and Y Talmon. Digital cryogenic transmission electron
42 microscopy: an advanced tool for direct imaging of complex fluids. *Colloids and Surfaces*
43 *A: Physicochemical and Engineering Aspects*, 183:113–122, 2001.
- 44
45 ²²Rose Omidvar, Alireza Dalili, Ali Mir, and Hadi Mohammadigoushki. Exploring sensitivity
46 of the extensional flow to wormlike micellar structure. *Journal of Non-Newtonian Fluid*
47 *Mechanics*, 252:48–56, 2018.
- 48
49 ²³François Lequeux. Reptation of connected wormlike micelles. *EPL (Europhysics Letters)*,
50 19(8):675, 1992.
- 51
52 ²⁴Lior Ziserman, Ludmila Abezgauz, Ory Ramon, Srinivasa R Raghavan, and Dganit
53 Danino. Origins of the viscosity peak in wormlike micellar solutions. 1. mixed cationic
54 surfactants. a cryo-transmission electron microscopy study. *Langmuir*, 25(18):10483–10489,
55 2009.
- 56
57 ²⁵Tanner S Davies, Aimee M Ketner, and Srinivasa R Raghavan. Self-assembly of surfactant
58 vesicles that transform into viscoelastic wormlike micelles upon heating. *Journal of the*
59 *American Chemical Society*, 128(20):6669–6675, 2006.
- 60
61 ²⁶Jinkee Lee, Amitesh Saha, Sabrina Montero Pancera, Andreas Kempter, Jens Rieger, Arijit
62 Bose, and Anubhav Tripathi. Shear free and blotless cryo-tem imaging: a new method for
63 probing early evolution of nanostructures. *Langmuir*, 28(9):4043–4046, 2012.
- 64
65 ²⁷Yi Zheng, Z Lin, JL Zakin, Y Talmon, HT Davis, and LE Scriven. Cryo-tem imaging
the flow-induced transition from vesicles to threadlike micelles. *The Journal of Physical*

- 1
2
3
4
5
6
7
8
9
10
11
12
13
14
15
16
17
18
19
20
21
22
23
24
25
26
27
28
29
30
31
32
33
34
35
36
37
38
39
40
41
42
43
44
45
46
47
48
49
50
51
52
53
54
55
56
57
58
59
60
61
62
63
64
65
- Chemistry B*, 104(22):5263–5271, 2000.
- ²⁸E Mendes, Janaky Narayanan, R Oda, F Kern, SJ Candau, and C Manohar. Shear-induced vesicle to wormlike micelle transition. *The Journal of Physical Chemistry B*, 101(13):2256–2258, 1997.
- ²⁹Yamaira I González and Eric W Kaler. Cryo-tem studies of worm-like micellar solutions. *Current opinion in colloid & interface science*, 10(5-6):256–260, 2005.
- ³⁰Michelle A Calabrese and Norman J Wagner. Detecting branching in wormlike micelles via dynamic scattering methods. *ACS Macro Letters*, 7(6):614–618, 2018.
- ³¹Noah H Cho, Qingteng Zhang, Eric M Dufresne, Suresh Narayanan, and Jeffrey J Richards. Microscopic dynamics of inverse wormlike micelles probed using x-ray photon correlation spectroscopy. *ACS Macro Letters*, 11(4):575–579, 2022.
- ³²Rose Omidvar, Shijian Wu, and Hadi Mohammadigoushki. Detecting wormlike micellar microstructure using extensional rheology. *Journal of Rheology*, 63(1):33–44, 2019.
- ³³Manojkumar Chellamuthu and Jonathan P Rothstein. Distinguishing between linear and branched wormlike micelle solutions using extensional rheology measurements. *Journal of Rheology*, 52(3):865–884, 2008.
- ³⁴Rossana Pasquino, Pietro Renato Avallone, Salvatore Costanzo, Ionita Inbal, Dganit Danino, Vincenzo Ianniello, Giovanni Ianniruberto, Giuseppe Marrucci, and Nino Grizzuti. On the startup behavior of wormlike micellar networks: The effect of different salts bound to the same surfactant molecule. *Journal of Rheology*, 67(2):353–364, 2023.
- ³⁵Samuel W Holder, Samuel C Grant, and Hadi Mohammadigoushki. Nuclear magnetic resonance diffusometry of linear and branched wormlike micelles. *Langmuir*, 37(12):3585–3596, 2021.
- ³⁶Peter Rasselov, Alfredo Scigliani, and Hadi Mohammadigoushki. Kinetics of shear banding flow formation in linear and branched wormlike micelles. *Soft Matter*, 2022.
- ³⁷Emmanuel Cappelaere and Robert Cressely. Influence of NaClO_3 on the rheological behaviour of a micellar solution of cpcl. *Rheologica acta*, 39(4):346–353, 2000.
- ³⁸E Cappelaere, JF Berret, JP Decruppe, R Cressely, and P Lindner. Rheology, birefringence, and small-angle neutron scattering in a charged micellar system: Evidence of a shear-induced phase transition. *Physical Review E*, 56(2):1869, 1997.
- ³⁹PJ Kreke, LJ Magid, and JC Gee. ^1H and ^{13}C nmr studies of mixed counterion, cetyltrimethylammonium bromide/cetyltrimethylammonium dichlorobenzoate, surfactant solutions: the intercalation of aromatic counterions. *Langmuir*, 12(3):699–705, 1996.
- ⁴⁰Chi-Yuan Cheng, Tatiana V Brinzari, Zhigang Hao, Xiaotai Wang, and Long Pan. Understanding methyl salicylate hydrolysis in the presence of amino acids. *Journal of Agricultural and Food Chemistry*, 69(21):6013–6021, 2021.
- ⁴¹Noriaki Funasaki, Seiji Ishikawa, and Saburo Neya. Proton nmr study of α -cyclodextrin inclusion of short-chain surfactants. *The Journal of Physical Chemistry B*, 107(37):10094–10099, 2003.
- ⁴²Oscar Ledea, Maritza Díaz, Jesús Molerio, Daniel Jardines, Aristides Rosado, and Teresa Correa. H-nmr spectroscopy study of oleic acid and methyl oleate ozonation in different reaction conditions. *Revista CENIC. Ciencias Químicas*, 34(1):3–8, 2003.
- ⁴³MR Lopez-Gonzalez, WM Holmes, and PT Callaghan. Rheo-nmr phenomena of wormlike micelles. *Soft Matter*, 2(10):855–869, 2006.
- ⁴⁴National Center for Biotechnology Information. Compound summary: Cetylpyridinium chloride, 2004.
- ⁴⁵Hugo E Gottlieb, Vadim Kotlyar, Abraham Nudelman, et al. Nmr chemical shifts of com-

- mon laboratory solvents as trace impurities. *Journal of organic chemistry*, 62(21):7512–7515, 1997.
- ⁴⁶Edward O Stejskal and John E Tanner. Spin diffusion measurements: spin echoes in the presence of a time-dependent field gradient. *The journal of chemical physics*, 42(1):288–292, 1965.
- ⁴⁷EO Stejskal. Use of spin echoes in a pulsed magnetic-field gradient to study anisotropic, restricted diffusion and flow. *The Journal of Chemical Physics*, 43(10):3597–3603, 1965.
- ⁴⁸R Mills. Self-diffusion in normal and heavy water in the range 1–45. deg. *The Journal of Physical Chemistry*, 77(5):685–688, 1973.
- ⁴⁹Ruggero Angelico, Samiul Amin, Maura Monduzzi, Sergio Murgia, Ulf Olsson, and Gerardo Palazzo. Impact of branching on the viscoelasticity of wormlike reverse micelles. *Soft Matter*, 8(42):10941–10949, 2012.
- ⁵⁰PT Callaghan, KW Jolley, and J Lelievre. Diffusion of water in the endosperm tissue of wheat grains as studied by pulsed field gradient nuclear magnetic resonance. *Biophysical journal*, 28(1):133–141, 1979.
- ⁵¹SC Grant, DL Buckley, S Gibbs, AG Webb, and SJ Blackband. Mr microscopy of multicomponent diffusion in single neurons. *Magnetic Resonance in Medicine: An Official Journal of the International Society for Magnetic Resonance in Medicine*, 46(6):1107–1112, 2001.
- ⁵²Christian Beaulieu and Peter S Allen. Determinants of anisotropic water diffusion in nerves. *Magnetic resonance in medicine*, 31(4):394–400, 1994.
- ⁵³Jonathan V Sehy, Joseph JH Ackerman, and Jeffrey J Neil. Evidence that both fast and slow water adc components arise from intracellular space. *Magnetic Resonance in Medicine: An Official Journal of the International Society for Magnetic Resonance in Medicine*, 48(5):765–770, 2002.
- ⁵⁴Ruggero Angelico, U Olsson, G Palazzo, and Andrea Ceglie. Surfactant curvilinear diffusion in giant wormlike micelles. *Physical review letters*, 81(13):2823, 1998.
- ⁵⁵Subas Dhakal and Radhakrishna Sureshkumar. Anomalous diffusion and stress relaxation in surfactant micelles. *Physical Review E*, 96(1):012605, 2017.
- ⁵⁶C Oelschlaeger, P Suwita, and N Willenbacher. Effect of counterion binding efficiency on structure and dynamics of wormlike micelles. *Langmuir*, 26(10):7045–7053, 2010.
- ⁵⁷Ashish V Sangwai and Radhakrishna Sureshkumar. Binary interactions and salt-induced coalescence of spherical micelles of cationic surfactants from molecular dynamics simulations. *Langmuir*, 28(2):1127–1135, 2012.
- ⁵⁸Durga P Acharya and Hironobu Kunieda. Wormlike micelles in mixed surfactant solutions. *Advances in colloid and interface science*, 123:401–413, 2006.
- ⁵⁹Horacio Cabral, Kanjiro Miyata, Kensuke Osada, and Kazunori Kataoka. Block copolymer micelles in nanomedicine applications. *Chemical reviews*, 118(14):6844–6892, 2018.

Alfredo Scigliani.: Data acquisition, data post processing, model fitting and analysis, writing original draft preparation. **Samuel C. Grant:** Implementing pulse sequences, methodology, reviewing and editing the manuscript. **Hadi Mohammadigoushki:** conceptualization, methodology, analysis of data, supervision, writing-reviewing and editing the manuscript.

Journal Pre-proofs

Declaration of interests

The authors declare that they have no known competing financial interests or personal relationships that could have appeared to influence the work reported in this paper.

The authors declare the following financial interests/personal relationships which may be considered as potential competing interests:

Journal Pre-proofs